

Grand canonical validation of the bipartite International Trade Network

Mika J. Straka,¹ Guido Caldarelli,^{1,2,3} and Fabio Saracco¹

¹*IMT School for Advanced Studies, Piazza San Francesco 19, 55100 Lucca, Italy*

²*Istituto dei Sistemi Complessi, CNR, Dip. Fisica Università “Sapienza”, P.le A. Moro 2, 00185 Rome, Italy*

³*London Institute for Mathematical Sciences, 35a South St, Mayfair London W1K 2XF, UK*

Devising strategies for economic development in a globally competitive landscape requires a solid and unbiased understanding of countries technological advancements and similarities among export products. Both can be addressed through the bipartite representation of the International Trade Network. In the present paper, we apply the recently proposed grand canonical projection algorithm to uncover country and product communities. Contrary to past endeavors, our methodology, based on information theory, creates monopartite projections in an unbiased and analytically tractable way. Single links between countries or products represent statistically significant signals, which are not accounted for by null-models such as the Bipartite Configuration Model. We find stable country communities reflecting the socioeconomic distinction in developed, newly industrialized, and developing countries. Furthermore, we observe product clusters based on the aforementioned country groups. Our analysis reveals the existence of a complicate structure in the bipartite International Trade Network: apart from the diversification of export baskets from the most basic to the most exclusive products, we observe a statistically significant signal of an export specialization mechanism towards more sophisticated products.

INTRODUCTION

The application of the network formalism in the field of socioeconomic science has seen an unprecedented growth in the last decades [1–3]. Most of our actions take place in network environments and neglecting such structures can lead to insufficient interaction models [4, 5] and poor policy regulation [6].

On the global scale, the analysis of the International Trade Network (ITN), also known as the World Trade Web, has taken a prominent role in the study of economic systems [7–10] motivated by the ongoing process of globalization. The ITN can be represented by a bipartite network in which the two layers are respectively countries and products [11, 12]: a link between the two layers is present if the selected country is able to export the chosen item. In this framework, [13, 14] proposed an algorithm that uncovers productive capabilities of countries, as well as the complexity of products.

Several works [15–17] proposed different algorithms to infer relations among products from this bipartite network. However, very often such methods are either too tailored to the problem at hand and therefore lack generalizability, or the observed similarity between products neglects the validation by a statistical null-model so that the signal is indistinguishable from the noise.

Surprisingly, few general methods for projecting bipartite networks are present in literature, among which the seminal method proposed in [18]. Call respectively L and Γ the two layers and suppose we want to project the bipartite network on the layer L ; according to this method, the original bipartite network is divided into slices that are homogeneous in the degree of nodes of the opposite layer Γ . Comparing the presence of actual links with uniform distributions in each slice permits to

establish the statistical significance of the observation and validate the co-occurrence of links between node pairs in the layer L . Even though this approach is poorly effective due to the high number of hypotheses to be tested (one for every couple of nodes in L for every slice), [18] defines a controlled framework in which a statistical analysis can be performed.

Recently, many efforts have been spent in providing an unbiased monopartite projection for bipartite networks [19–21]. Summarizing, through the comparison of the actual measurements with the expectations of the Bipartite Configuration Model (BiCM, [22]), it is possible to state if a node couple belonging to the same layer share a statistically significant fraction of their connections. In this process the BiCM may be too “strict” and could account for all the observations in the data [21]: otherwise stated, the method may be too effective in reproducing original data. Although the original proposal embeds the BiCM [19–21], the framework is very general and nothing prevents from using “weaker” null-models [21].

In the present paper, we apply the aforementioned approach (discussed in details in [21]) to the International Trade Network. The Configuration Model class is essentially obtained from entropy maximization and, since their derivation follows the general approach of [23], we will refer to this method as the *grand canonical projection algorithm*.

We observe that the BiCM induces a community structure which largely agrees with the socioeconomic distinction between developed, newly industrialized, developing and mainly raw material exporting countries. Our analysis reveals a division within the group of developed countries around year 2000 into a core (Germany, USA, Japan, France, etc.) and a periphery (Austria,

Italy, Spain, Eastern European countries, etc.), with the latter acting as a bridge to developing countries.

The grand canonical projection shows also the presence of communities of products, which essentially reflect the development of their exporters. In particular, technological chemistry products cluster together because they are exported by the same developed countries, whereas electronic devices, textiles and garments form a community since they represent the typical exports of newly industrialized and developing countries. Each community of countries occupies the projected network of products in a particular way, focusing their efforts on few product communities, thus implying the presence of a statistically significant signal of specialization. Note that, usually, the picture arising from the analysis of the bipartite ITN is interpreted as the fact that the most developed countries export literally all possible products. In the present article, we refine this picture by highlighting that developed countries focus more on the most complex, i.e. technologically advanced, goods. A similar signal was already mentioned in the supplementary information of [22], though not discussed in details: the observed network appeared much more disassortative than the randomization, implying that countries with the largest export baskets link more than expected to products with the highest complexities, i.e. with the lowest degrees. These new results put in relation the topological network structure with economical meaning of the case study considered.

The paper is organized as follows. Firstly, we briefly introduce the ingredients of the grand canonical projection algorithm in the Methods section; more details on the BiCM and on the projection technique of the original article [21] are provided in the Appendix A. The Results section presents the monopartite projections obtained from different null-models and their composition in terms of country communities, which reflect their stages in economic development, as well as product communities, based on their technological sophistication. Finally, we comment on the results and the performance of the methodology in the Conclusions.

METHODS

We consider a binary bipartite network composed of two distinct node sets and a collection E of undirected and unweighted edges. In the following, we distinguish the nodes sets by using Latin and Greek indices. The bipartite network is described by a binary biadjacency matrix M of dimension $N_i \times N_\alpha$, where N_i and N_α are the dimensions respectively of the Latin and the Greek layer and an edges between node couples (i, α) is represented by the matrix entry $M_{i\alpha} = 1$.

In a bipartite network, the similarity between two nodes of the same layer is usually measured by the number of nearest neighbors in the opposite layer. Even though this method is direct and intuitive, it neglects the crucial problem of determining which edges contain statistically relevant information and which do not. To address this question, in the present paper we employ the grand canonical projection methodology proposed in [21], since it provides exact results and a coherent formalism. In the following, we will briefly review the method, inviting the interested reader to the original article.

Grand canonical projection

The grand canonical projection algorithm proposed in [21] yields a statistically validated monopartite projection of a bipartite network by comparing the observed node similarities with the expectations from a suitable null-model.

Bipartite motifs as a measure of similarity The number of common neighbors shared by two nodes of the same Latin (Greek) layer can be used as a measure of similarity. In the literature this quantity is known as the number of $K_{2,1}$ ($K_{1,2}$) bi-cliques [24] or, following the formalism of [22], as the number of V-motifs (Λ -motifs). Fig. 1 illustrates the V-motifs between nodes i and j . The

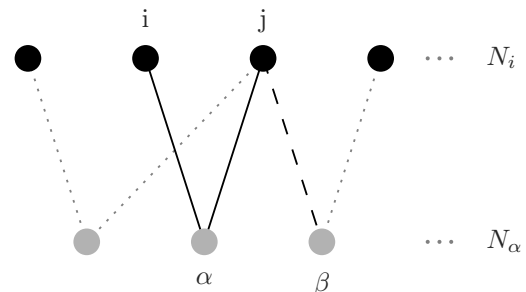


Figure 1: The V_α^{ij} -motif is illustrated by the bold black edges between node couples (i, α) and (j, α) .

Analogously, the edges between (j, α) and (j, β) describe the $\Lambda_{\alpha\beta}^j$ -motif. The top layer contains the “Latin” nodes, the bottom the “Greek” nodes. Other edges are indicated by dotted gray lines.

total number of V-motifs between these nodes is

$$V^{ij} = \sum_{\alpha} V_{\alpha}^{ij} = \sum_{\alpha} M_{i\alpha} M_{j\alpha}. \quad (1)$$

Bipartite Configuration Model and Bipartite Partial Configuration Models In order to establish whether two

nodes are similar in a statistical sense, we compare the V-motif abundances with their expectations from the Bipartite Configuration Model (BiCM, [22]). The BiCM is an entropy based null-model in which the information of the degree sequence of both layers is discounted. It has been shown [11–17, 22] that the degree sequence is able to capture much of the structure of the bipartite international trade, as the triangular nested shape of the biadjacency matrix. Hence, discounting the degree sequence with a null-model allows to uncover more detailed substructures, which are otherwise hardly observable.

The method is composed of two main steps: entropy maximization and likelihood maximization. In the first step, we define \mathcal{G}_B , an ensemble of bipartite graphs in which the number of links can vary and the number of nodes per layer is fixed to the value of the network under analysis. We define the Shannon entropy of the ensemble as

$$S = - \sum_{G_B \in \mathcal{G}_B} P(G_B) \ln P(G_B),$$

where $P(G_B)$ is the probability of observing graph $G_B \in \mathcal{G}_B$.

The choice of the Shannon entropy is standard in information theory and implicitly assumes that the system is ergodic, i.e. that all link configurations are theoretically possible. For non-ergodic or non-Markovian systems, the use of a non-additive entropy definition is recommended [25, 26]. In principle, different entropies could also be implemented in our case, although it has been shown that the Shannon entropy outperforms other entropy functionals in the context of behavioral networks [27] in recovering missing information.

In the BiCM, we want to maximize the entropy constraining the degree sequence of both layers. Call k_i and k_α the degrees of the node i and α , defined respectively on the Latin and the Greek layer, and θ_i and θ_α their relative Lagrangian multipliers. After the entropy maximization, the probability per graph reads

$$P(G_B | \theta_i, \theta_\alpha) = \prod_{i, \alpha} \frac{e^{-(\theta_i + \theta_\alpha)}}{1 + e^{-(\theta_i + \theta_\alpha)}}$$

(see Appendix A for more details).

The graph probability is a function of the unknown Lagrangian multipliers θ_i and θ_α . They can be estimated by maximizing the likelihood $\mathcal{L} = \ln P(G_B | \vec{\theta})$ of observing the real network. It is possible to show that this approach is equivalent to imposing that the expectation values over the ensemble of the degree sequences are equal to those of the real network:

$$\begin{cases} \langle k_i \rangle = \sum_\alpha \frac{e^{-(\theta_i + \theta_\alpha)}}{1 + e^{-(\theta_i + \theta_\alpha)}} = k_i^*; \\ \langle k_\alpha \rangle = \sum_i \frac{e^{-(\theta_i + \theta_\alpha)}}{1 + e^{-(\theta_i + \theta_\alpha)}} = k_\alpha^*, \end{cases}$$

The values measured on the real network are marked with asterisks (*). By solving the previous equations for θ_i and θ_α , it is possible to obtain the explicit value of the probability per graph in the ensemble.

One of the most powerful properties of the BiCM is that it provides independent probabilities per link, which in turn permits to readily calculate the expectation values of more complicated quantities. For instance, the average number of V-motifs between i and j is

$$\langle V^{ij} \rangle^{\text{BiCM}} = \sum_\alpha p_{i\alpha}^{\text{BiCM}} p_{j\alpha}^{\text{BiCM}}, \quad (2)$$

where $p_{i\alpha}^{\text{BiCM}}$ is the probability of observing a link between nodes i and α according to the BiCM.

Note that we could also impose non-linear constraints, such as the degree variance of each node. However, this would lead to non-independent link probabilities and complicate expressions such as eq. (2) significantly. Nevertheless, discounting the information of more elaborate constraints, for example the bipartite clustering, may reveal other non-trivial structures. Constraining the degree sequence thus represents a trade-off between discounting non-trivial information and providing transparent and easy-to-use tools for the analysis of bipartite networks.

In the following, we compute the expected values of the bipartite motifs presented in the previous paragraph according to the BiCM. For the present objective, the constraints may turn out to be too strict, meaning that they capture the main information contained in the network and no statistical significant signal can be seen. In this case, it is opportune to relax the constraints and fix the degrees of just a single layer. This model has been proposed as the Bipartite Partial Configuration Model (BiPCM, [21]). Implicitly, the BiPCM_i, i.e. the one in which only the degree sequence of the Latin layer is captured, is equivalent to a BiCM in which all nodes in the Greek layer have degrees equal to their mean. The BiPCM_i is more effective in reproducing the observed number of V-motifs rather than the number of Λ -motifs. Intuitively, the degrees of the nodes i and j carry more information about V_{ij} than the node degrees of the opposite layer. Analogously, the BiPCM _{α} reproduces Λ -motifs better than V-motifs.

In some cases, the projection of the real bipartite network can be completely reconstructed from its (bipartite) degree sequence, which means that the BiCM would be too strict to validate any links in the projection algorithm. The use of the BiPCM is thus recommended. By neglecting the information contained in the degree sequence of the layer opposite to the one of the projection, the BiPCM allows for stronger fluctuations stemming from the heterogeneity of the degrees which can be captured by the projection. A unique criterion for deciding a priori which null-model is more effective is currently missing as we are examining the limits of the

different projections. This notwithstanding, as a rule of thumb we suggest that the BiPCM should be used when one deals with bipartite layers of very different lengths ($\frac{\text{longer layer}}{\text{shorter layer}} \gg 1$) and one intends to project on the longer layer. Since the variability of the bipartite motifs is determined by the opposite layer, which is much shorter in this case, the BiCM is likely not to validate any links. In all other cases, the BiCM should be preferred.

In the literature, the recent Curveball algorithm offers another way to discount the degree-sequence information in an unbiased null-model for bipartite networks. [28]. The authors implement a degree-sequence-preserving rewiring algorithm in order to build the ensemble of networks explicitly. Remarkably, the method is ergodic, i.e. it explores the phases space uniformly [29] (note that the ergodicity of BiCM is automatically obtained by construction). Although the algorithm is relatively fast, the fact that it is micro canonical does not permit to calculate the expectation values of different quantities, thus preventing the possibility of writing an expression like eq. (2). In fact, $\langle V^{ij} \rangle^{\text{Curveball}}$ can be estimated as the average over a sample of the original ensemble defined by the Curveball algorithm. However, this sample has to be big enough in order to provide a sufficient statistics, i.e. to represent at best the whole ensemble without losing its statistical properties. For big networks, this procedure implies the presence of a large sample, which is hard to handle and increases the calculation times dramatically.

Statistical significance of node similarities: p -values and False Discovery Rate Both, the BiCM and the BiPCM, provide closed forms for the probability distributions of the Λ - and V -motifs. In the case of the BiCM, they follow a generalization of the binomial distribution, called Poisson-Binomial distribution [30–32], for each node couple. Depending on the constrained layer, the BiPCMs provide different distributions: for BiPCM _{i} , V -motifs follow a different Binomial distribution for each couple (i, j) , whereas the Λ -motif distribution is the same Poisson-Binomial distribution for every couple (α, β) . The contrary happens for BiPCM _{α} .

By comparing the observed bipartite motifs with their null-model expectations, it is possible to calculate their associated p -values, i.e. the cumulative probability of observing a value greater than or equal to the one actually observed. In a nutshell, the smaller the p -value, the larger the similarity between the respective nodes compared to the null-model expectation. In order to validate the links between all the node couples in the same layer, a multiple hypotheses testing procedure should be adopted. In this framework, it is common to control the False Discovery Rate (FDR), i.e. the rate of falsely rejected null hypotheses [33]. Finally, the

projection network can be obtained by drawing links whose p -values is statistically significant according to the FDR test. In the following, the significance level of all validated networks is $\alpha = 0.01$.

We created an open-source implementation of the null-models and the calculation of the p -values in Python, which are freely available on the web [34]. More details on the bipartite configuration models, the similarity measures and their distributions can be found in Appendix A.

DATA

We use the BACI HS 2007 database from CEPII [35] to construct the bipartite network, which comprises the export data for the years 1995 - 2010. Products are identified according to the Harmonized System and organized in hierarchical categories at different aggregation levels, which are captured by two, four, or six digit product codes. Here, we adopt the 2007 code revision (HS 2007) with four digit codes describing 1131 different products. In order to binarize data, it is customary to apply the revealed comparative advantage (RCA), also referred to as Balassa index [36], which describes whether a specific country is a relevant exporter of a product ($RCA \geq 1$) or not ($RCA < 1$) by comparing the relative monetary importance of the product in the country's export basket to the global average. The RCA is defined as

$$RCA_{c,p} = \frac{e(c,p)}{\sum_{p'} e(c,p')} \bigg/ \frac{\sum_{c'} e(c',p)}{\sum_{c',p'} e(c',p')}, \quad (3)$$

where $e(c,p)$ denotes the export value of product p in country c 's export basket.

Basic properties of the binary biadjacency matrix of the ITN

In the bipartite ITN, the degree distributions resemble a power-law for the countries and a Gaussian for the products. The degree heterogeneity can be approximately captured by the coefficient of variation (CV), i.e. the standard deviation over the mean, $\frac{\sigma}{\mu}$. As a rule of thumb, the larger the CV the less informative is the mean about the whole distribution.

The probabilities per link of the partial model BiPCM _{i} (BiPCM _{α}) are those of the BiCM in which the degree sequence of the opposite layer is approximated by its mean, i.e. $\langle k_\alpha \rangle = \frac{|E|}{N_\alpha}$, $\forall \alpha$ ($\langle k_i \rangle = \frac{|E|}{N_i}$, $\forall i$), where $|E|$ is the total number of edges. Since the CV varies between 0.5 and 0.55 for the products and between 0.82 and 0.89 for the countries, the BiPCM _{i} will reproduce the V -motifs better

between the countries than the BiPCM_α the Λ -motifs between the products. Generally speaking, the approximation implied by the partial null-models will work best for small CV and lose accuracy as the CV increases.

In the trade data set we examine, the number of products is almost 10 times the number of countries and the biadjacency matrix is hence strongly rectangular. The connectance varies during the years between 0.09 and almost 0.13. This feature is related to the division of products in categories (see, for instance, [37]).

RESULTS

The degree sequences of the binary bipartite trade network represent the sizes of country export baskets and the number of exporters of products, respectively. Implementing a null-model which discounts the information from the degree sequence (e.g. BiCM and BiPCM) implies focusing on structures that are not already contained in the heterogeneity of the degree distribution. For instance, in the BiCM the US export basket keeps its size while the composition of export products within the basket is randomized. In the following, we shall observe effects in the structure of the international trade that are not explainable from dishomogeneities of the degree sequences alone.

Country layer projection

The projection on the country layer induced by the BiCM reveals important information on different levels of economic development and the roles played by various countries in the globalization process.

As shown in Fig. 2, an enhanced version of the Louvain community detection algorithm [38] applied for the various years produces four stable clusters: developed countries (blue/dark gray), newly industrialized countries (light purple/lighter gray), African and South American developing countries (green/darker gray); developing countries exporting mainly raw materials such as oil (orange/light gray). Despite some noise from year to year, mayor representatives of the blue community are Germany, USA, Japan, UK, and other European countries, while the purple community comprehends China, India, Turkey, Southeast Asia and some Central American countries; in the cluster of raw material exporters Russia, Saudi Arabia, Venezuela, post-Soviet states and North African countries can be found.

Furthermore, we discern a fifth group whose composition fluctuates strongly during the considered time interval. It is mainly composed of countries with large coastal regions, which have little access to neighboring countries via continental trade routes. The community includes, among others, Australia, New Zealand, Canada, Chile,

and Argentina. Much of their industrial output is aimed at internal markets and exports are strong in the fishing sector, especially for Canada and Chile. This explains why they are loosely linked to poorly industrialized nations like Mauritania, whose most important trade goods derive from fishing activities. As a result of the weak connectivity within the group, countries oscillate between different communities, which can clearly be seen, for example, for Australia and Canada in Fig. 2.

Relaxing the conditions of the null-model to just the degree sequence of the country layer leads to the BiPCM_c -induced projection. The community structure is more stable than for the BiCM. In particular, note

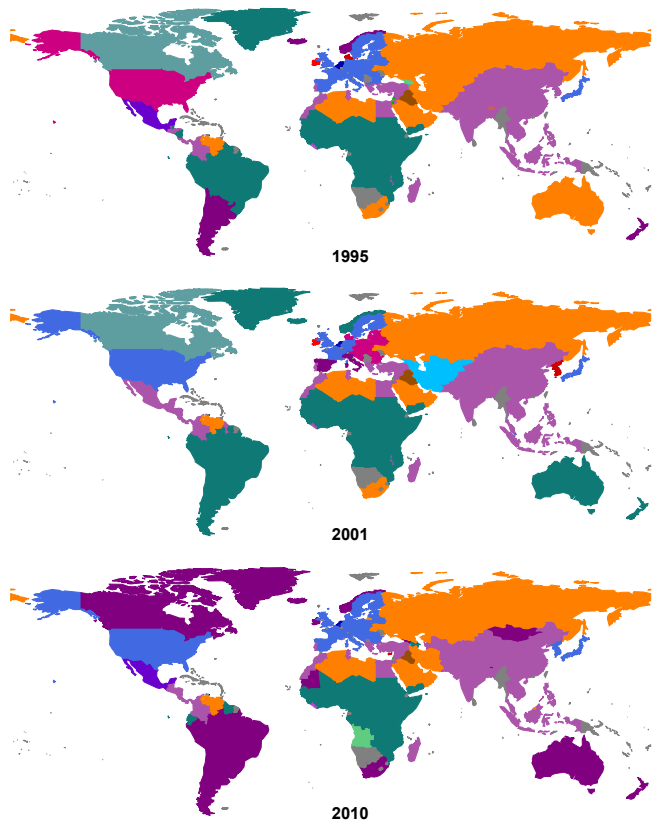


Figure 2: Communities of countries based on BiCM projection for the years: 1995, 2001, 2010. Even though the division in communities show some noise, the partition in the following communities is stable: developed countries (blue/dark gray, see central Europe), newly industrialized and developing countries (light purple/lighter gray, see China), developing countries (green/darker gray, see central Africa), and countries whose exports rely on raw materials, e.g. oil (orange/light gray, see Russia).

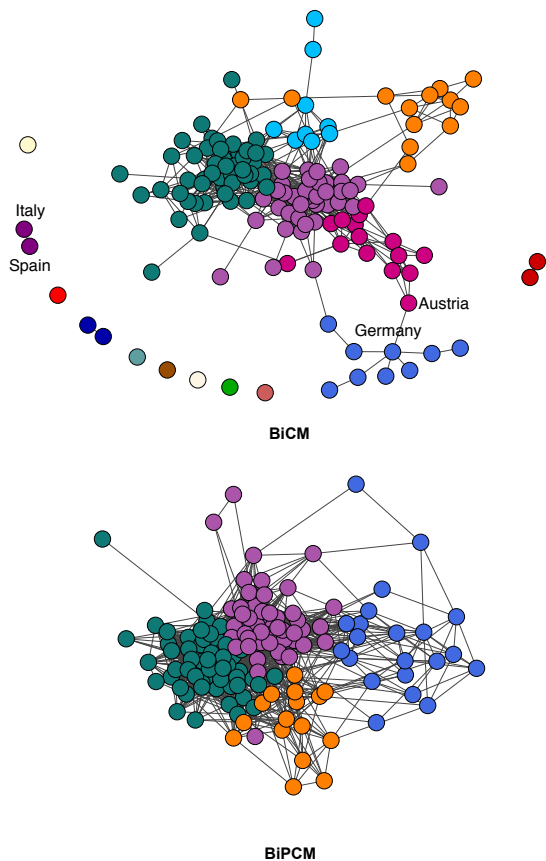


Figure 3: Structure of the projected country network obtained with the BiCM and the BiPCM_c for the year 2001. Note that in weakening the constraints, i.e. passing from BiCM to BiPCM_c, the connectance increases.

in Fig. 4 that the fluctuating community disappears and the division of countries is more static. Weakening the constraints of the null-model thus reduces the noise in the projection. As a matter of fact, neglecting the constraints on the product layer means considering just the mean of the product degree sequence. The approximation is more accurate the smaller the relative dispersion of the product degrees, which is captured by the coefficient of variation and amounts to $CV \sim 0.5$ in the present case (see “Data” section).

The downside of the stability of the BiPCM_c projection is that it covers small, but insightful, structural changes. For instance, the BiCM manages to capture the split-off of Italy and Spain from the developed countries, as well as the separation of the developed European countries in an Eastern and a Western part during the years 1997-2002. As can be seen in Fig. 3, Germany and Austria form a bridge between the Western and Eastern nations, with the latter themselves connecting to developing

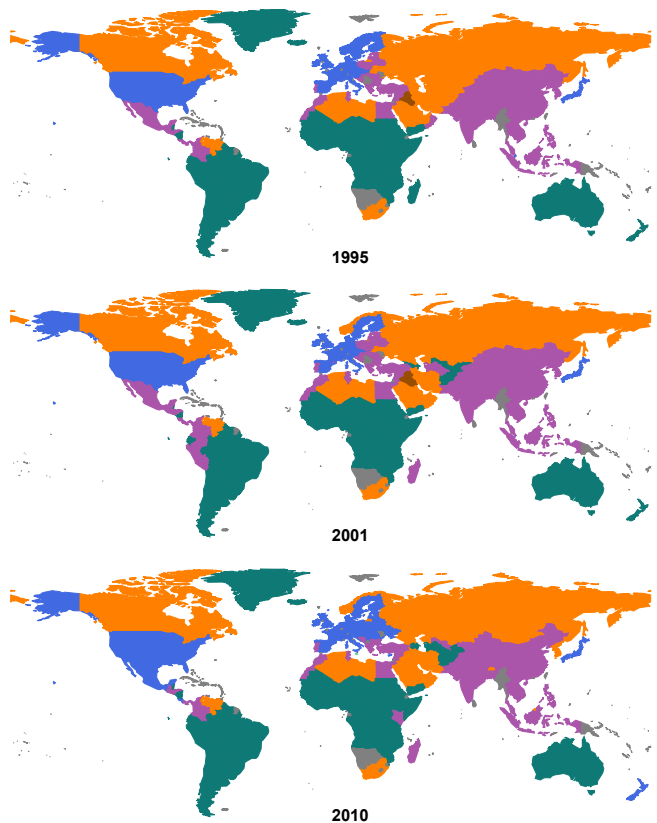


Figure 4: Country communities based on the BiPCM_c projection for the years: 1995, 2001, 2010. Compared to the BiCM communities of Fig. 2, the partition here is more stable.

countries.

Another striking result of the analysis of the country projection is the fact that many post-Soviet states still share a similar economic development years after the dissolution of the Soviet Union. A similar signal was detected in [39].

Product layer projection

The BiCM-induced projection of the bipartite ITN network on the product layer does not reveal any statistically significant links, as already mentioned in [21]. In other words, the total degree sequence of both countries and products contains enough information to account for the observed product similarities in terms of the Λ -motifs.

This observation stands in stark contrast to the country projection and is mainly due to two reasons connected to the different cardinalities of the layers. Firstly, the

effective p -value threshold for the validation procedure is proportional to the ratio of the significance level α over the number of tests that have to be performed, i.e. $\propto \alpha/\binom{N}{2}$ for N nodes, as shown in Appendix A. Hence, the statistical validation is more restrictive on “longer” layers. In our case, the product layer is almost ten times larger than the country layer, which leads to a comparatively smaller effective threshold level. Secondly, the variability of node degrees depends on the length of the opposite layer, as mentioned in the Methods section, since the degree of each node stays in the interval between one and the dimension of the opposite layer. The degree heterogeneity of the longer layer is thus generally more limited than the one of the shorter layer, which reduces the set of possible values of the bipartite motifs between products in the present case.

Due to the behavior of the BiCM, we implemented the BiPCM_p to perform the validation procedure for product similarities. As mentioned in the Methods section, constraining product degrees is more effective in reproducing the Λ -motif distribution than constraining country degrees. However, BiPCM_p is going to be less effective in reproducing Λ -motifs than BiPCM_c in reproducing V -motifs, since the coefficient of variation for the countries $CV \simeq 0.8$ indicates a higher loss of information when approximating the country degree sequence by its mean.

The BiPCM_p-induced product networks are sparse with connectances in the range of 0.009-0.013 and highly fragmented for the years 1995-2010. As shown by the Jaccard indices of the edge sets in Fig. 6, they are quite dissimilar from year to year. In the country networks on the contrary, the value never falls below 0.75 and 0.8 for the BiCM and BiPCM_c, respectively. Nevertheless, the signal of product similarity persists: in fact, the enhanced Louvain community detection algorithm discovers a community structure that is stable throughout the years. The projection pinpoints evidently close relationships and captures broad communities, which remain constant, although the single links do not.

Going into detail, the BiPCM_p network consists of many small clusters surrounding the largest connected component (LCC), see Fig. 5 [40] for the year 2000. Most of the isolated clusters are composed of vegetables, fruits, and their derivatives, such as lettuce and cabbage, soybeans and soybean oil, or fruit juice and jams. Other connections are less trivial: lead ores and zinc ores, for instance, are typically present in the same geological rock formations and appear as an isolated component in the network.

The community detection algorithm uncovers a rich community structure inside the LCC, as shown in Fig. 5 for the year 2000. In the outer regions of the LCC we observe well-defined clusters, the most prominent

of them being the garment and textile cluster that contains clothes and shoe products. Furthermore, one can discern a distinct community containing electrical equipment, such as circuits, diodes, telephones, and electrical instruments. Other clusters comprise bovine and fish products, yarns and fabrics, and goods made out of wood, such as planks, tool handles, etc.

The core of the LCC, on the other hand, hosts several overlapping communities containing mostly more sophisticated products, such as motors and generators, machines, cars, turbines, arms, chemical products, antibiotics, and other industrial products. The community compositions are subject to fluctuations and include also, for example, agriculture and dairy products. The fuzziness of the core communities is due to the fact that they are typically exported by “developed” countries, which have large exportation baskets [11–14].

Note that the product communities do not follow necessarily the HS 2007 categorization, which is evident for the core communities where commodities of different origins can be found. As depicted in Fig. 5, the green community, for example, is formed by milk, heavy-duty vehicles, and metal pipes. Although this may seem confusing at first sight, it is largely due to the fact that the projection derives originally from the exportation network and should reflect the different levels of industrialization of the exporting countries. This behavior is shown in Fig. 7: different country communities occupy mostly different product communities, as is captured by the index $I_{CP} = \frac{\sum_{i \in C, \alpha \in P} M_{i\alpha}}{|C||P|}$, i.e. the density of links between country community C and product community P [21]. Developed countries focus on the core communities and export, for instance, highly technological machinery and sophisticated chemical products. At the same time, however, their export baskets encompass also products of low complexity such as milk and pipes, which are also exported, in fact, by newly industrialized countries next to textile products, garments, etc. In other words, the communities we observe, both on the product and the country layer, are derived from the way items interact: similar exports define countries with similar industrial development and, on the other hand, similar exporters define product communities of comparable technological level.

The relative focus of country communities on specific product groups has strong implications. Evidence presented in studies on the bipartite representation of international trade [11–17, 41] connect productive capabilities to the triangular shape of the country-product biadjacency matrix, advocating that the most developed countries export even the least complex products. This stands in contrast to standard economic theories

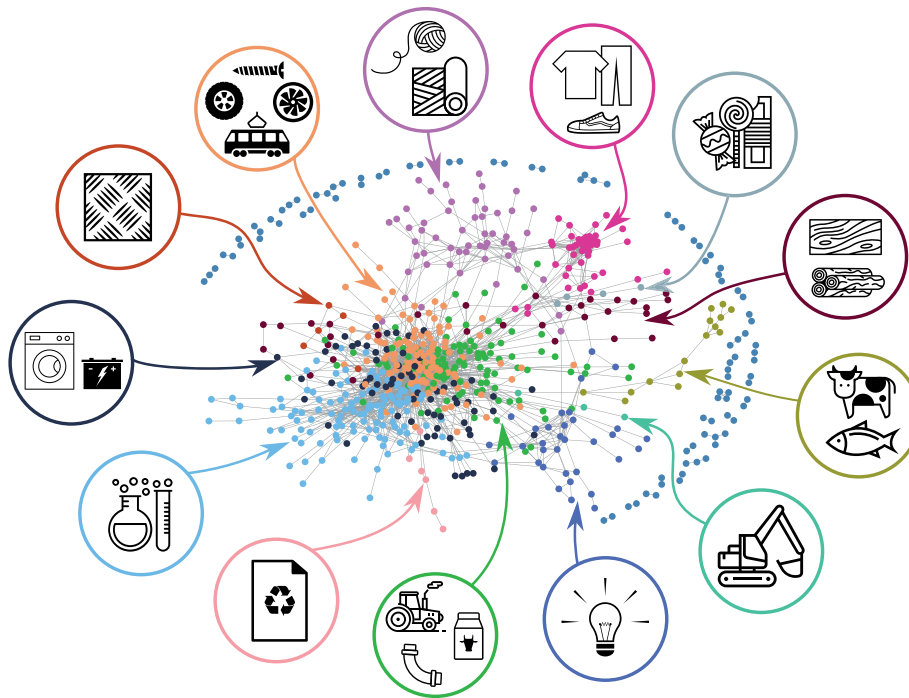


Figure 5: BiPCM_p product network spanned by FDR validated edges for $\alpha = 10^{-2}$ in the year 2000. The communities have been obtained using the Louvain algorithm and include the following products, starting on the top and going clockwise: • fabrics, yarn, etc.; • clothes, shoes, etc.; • wooden products; • animal products; • basic electronics; • chemicals; • machinery; • advanced electronics and machinery.

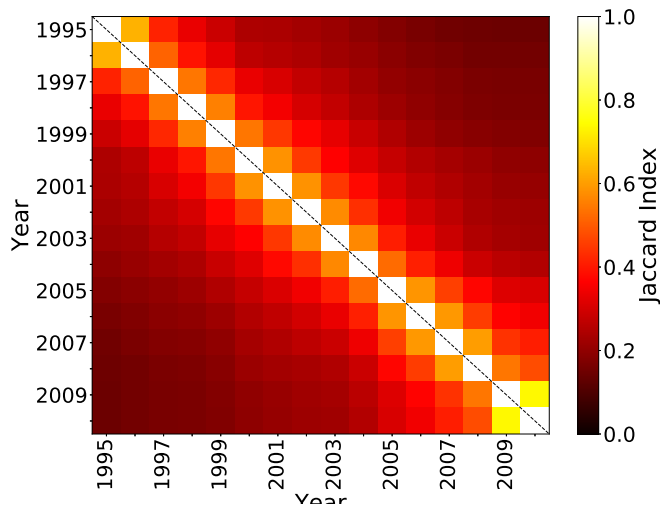


Figure 6: Comparison of the product networks for the years 1995-2010. The Jaccard index measures the similarity between their edge sets, E , and is defined as $|E_{year_i} \cap E_{year_j}| / |E_{year_i} \cup E_{year_j}|$. The values fall very quickly below 0.5 for $|year_i - year_j| > 2$.

expressed by Ricardo [42]: according to his hypothesis,

every country should specialize on the production of the most sophisticated goods its resources can support, even if they would be able to export less elaborate items as well.

In past studies, the Configuration Models demonstrated their ability to uncover sub-structures and less evident information [39, 43]. Already in [22] it was mentioned that the actual trade network is more disassortative than expected from the BiCM, implying that high degree countries (i.e. the ones with the largest export baskets) tend to export low degree products (i.e. the most exclusive and sophisticated ones) more than expected from the randomization.

Figure 7 explicitly shows that different countries, based on their technological level, tend to focus of different areas of the product network. Otherwise stated, even if the biadjacency matrix is triangular, still, once discounted the contribution of the dimension of export baskets and the number of exporters, a statistically significant signal shows the presence of industrial specialization. In order to highlight this phenomenon, we compare the link densities in the biadjacency matrix with the expectations from the BiCM null-model. For every entry in the matrix, we consider a box of 20 countries \times 80 products that surrounds it [44]. We quantify the discrepancies between the observed number of links in

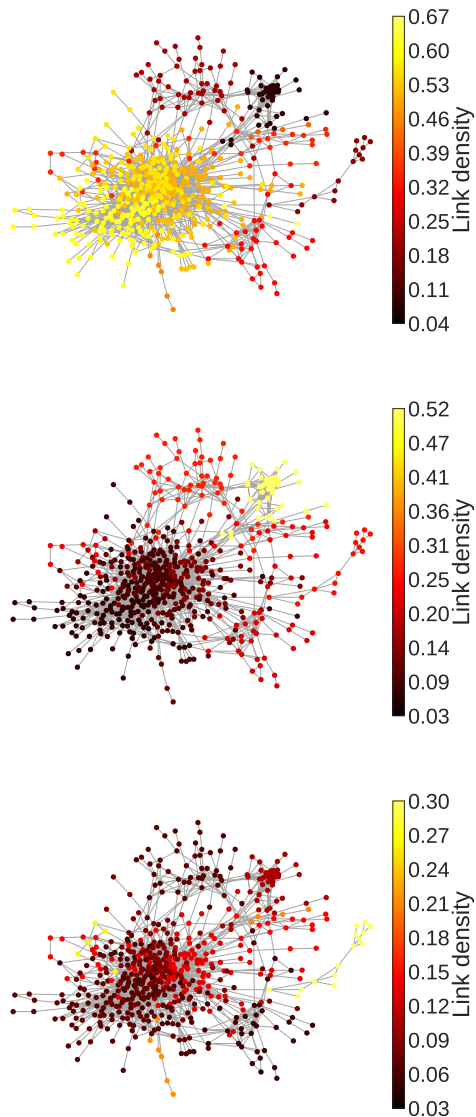


Figure 7: The images show the relative focus of the country communities’ exportation on different product cluster of the BiPCM_p product network for the year 2000. Top: developed countries occupy the central communities of high technological and chemical products. Middle: developing countries focus on peripheral communities with relatively low complexity [13, 14]. Bottom: raw material exporters are comparatively less focused, as shown in the link densities.

the boxes and their expectations from the BiCM using z-scores, i.e. $z_{\text{BiCM}}(x) = \frac{x - \langle x \rangle_{\text{BiCM}}}{\sigma_{\text{BiCM}}(x)}$. Z-scores express the difference between the real value and the expectation in terms of the standard deviation: $z \ll -3$ indicates that the observation is (significantly) less than the null-model expectation, whereas $z \gg 3$ is (significantly) more. In

Fig. 8 we represent the z-scores as a heat map on top of the country-product biadjacency matrix. Links are shown as white dots. “Hotter” (lighter) areas are those where the actual number of links significantly exceeds the BiCM expectation, whereas “colder” (darker) areas are those with less links than expected. It is possible to observe two hot areas in the top left and bottom right corner. The former shows that low fitness countries export basic products much more than expected ($z \sim 25$), whereas the latter highlights the tendency of developed countries to export sophisticated products ($z \sim 15$). Contrary to that, the bottom left corner illustrates that high fitness countries export basic products much less than expected ($z \sim -20$). It is possible to observe a “hot” area stretching from the top left to the bottom right just below the diagonal of the matrix and a “cold” one just below that, highlighting the tendency of countries to focus on the most sophisticated products they are able to export.

CONCLUSIONS

In the present paper we analyze the relations among countries and among products in the bipartite representation of the international trade network (ITN) [11–16] by implementing a recently proposed strategy for the projection of bipartite networks [19–21]. The method is based on the Bipartite Configuration Model [22], an entropy-based null-model discounting the information of node degrees. As a matter of fact, it has been shown that the degree sequence is responsible for the main characteristics of the trade network, such as the triangular structure of the biadjacency matrix between countries and products, see Fig. 8, [11–17, 41] Using the BiCM as a filter permits to uncover structures of the network not explained by node degrees.

The application of the BiCM to the ITN as a statistical null-model reveals communities of countries with similar economic development, namely developed, newly industrialized, and developing countries, and raw material (e.g. oil) exporters. These groups are stable throughout the years 1995-2010 except for some small deviations due to different progress in the ongoing globalization process. The communities become even more stable using the BiPCM (a weaker version of BiCM in which the degree sequence of only a single layer is constrained) for the monopartite projection. At the same time, however, the BiPCM is not able to detect smaller details like, for example, the post-Soviet state community, which is instead captured by the BiCM.

Regarding the product layer, the BiCM turns out to be too restrictive to uncover any significant product similarities. In other words, the information contained in the degree sequence of both layers is enough to account for the observed product relations in the data.

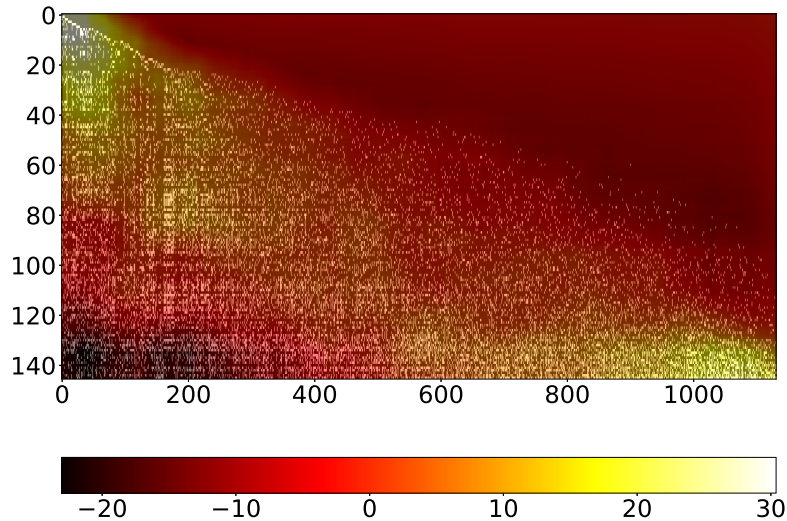


Figure 8: Representation of the biadjacency matrix for the year 2000 with countries along the rows and products along the columns, ordered by ascending fitness and complexity ranking, respectively [13, 14]. Links are shown as white dots. The superimposed colors (gray shading) correspond to the z-scores of the connectivity with respect to the BiCM. The z-scores are calculated for boxes containing 20 countries and 80 products which are centered on the respective matrix entry. Lighter colors indicate a higher presence of links than in the random null-model, darker shades a lower one. As can be seen in the lower right corner, the most developed countries (i.e. the bottom rows in the figure with the largest export baskets) have higher densities that exceed the expectations from the null-model for the most sophisticated products, i.e. those with the fewest exporters ($z \sim 15$). On the other hand, the least developed countries with the smallest export baskets focus their exports on basic products ($z \sim 25$), as shown in the upper left corner. In addition, the lower left part of the matrix shows that high fitness countries export low complexity products much less than would be expected from the BiCM. This indicates that countries export as many products as they are capable of while focusing their efforts on the most sophisticated commodities at the same time.

Investigating the similarity among products therefore requires a relaxation of the constraints, logically leading to the application of the BiPCM. Such a phenomenon is essentially due to the rectangularity of the biadjacency matrix, i.e. to the dimension of the support of the distribution of bipartite motifs (for details see the Methods section).

Using the BiPCM, we find product communities which define different industrialization levels and reflect the economic stages of their exporting countries. Highly sophisticated chemical products distinguish developed from newly industrialized and developing countries, whose exports focus mainly on electronic articles like diodes and telephones, or textiles and garments. It is worth pointing out that the communities are generally not due to productive chains, which should be reflected in a tree-like organization of the network. Observed clusters suggest that they are rather defined by the way

countries organize their export baskets.

Remarkably, our methods reveals a deeper structure than those discussed in [11–17, 41]. As already observed in previous studies, the biadjacency matrix of the country-product ITN is approximately triangular, which highlights the tendency of developed countries to export all possible products and not just the most exclusive ones. This observation conflicts with the Ricardo hypothesis, according to which countries should specialize their production on the most sophisticated products according to their resources.

However, as already mentioned, but not fully discussed, in the supplementary material of [22], the real network appears more disassortative than expected by discounting the degree sequence. Otherwise stated, countries with a larger export basket tend to export more sophisticated products than expected. In the present paper we fully observe such a phenomenon

through the different occupation patterns of product networks: different country communities with different technological levels tend to organize their export baskets differently, as shown in Fig. 7.

The heat map in Fig. 8 shows this phenomenon directly on the biadjacency matrix. The colors represent the z-scores encoding the discrepancy between the number of observed links in boxes drawn around the matrix entries and their expectations derived from the BiCM null-model (results are independent on the dimension of the box). Lighter colors represent abundances of links that are not explained by the null-model, whereas darker colors illustrate a lack in the links. Fig. 8 shows that countries do not abandon the production of the most basic products, although they focus their exports on the most exclusive products. This can be seen by the “hotter” areas close to the diagonal, i.e. for the most exclusive products in the countries’ export baskets. One can argue that the Ricardo hypothesis appears as a sort of second order effect: at first order the structure of the biadjacency matrix shows that the most developed countries are those with the largest export baskets (not those focused on most exclusive ones), at the second order a tendency to specialization is visible through a denser area for the most sophisticated products in the export basket.

In summary, the grand canonical projection algorithm uncovers subtle structures in the network under analysis: in the case of the world trade web, it reveals an industrial specialization effect of country exports which is not appreciable without the implementation of a null-model. This observation reconciles the apparent contrast between recent studies that describe the development of national productive capabilities in terms of the size of the export baskets on the one hand, and standard economics and the Ricardo hypothesis expecting an industrial specialization on increasingly complex products on the other hand. From our analysis we can conclude that the degree sequence of the bipartite network is responsible for the triangular shape of the country-product biadjacency matrix, and thus for the former, whereas the specialization effect is uncovered only once this information is discounted with the help of an appropriately defined null-models. It is worth mentioning that both the differentiation and specialization of countries are global and present throughout the whole period of the analyzed data set. As shown in Fig. 2, local dynamics are observed through changes in the community compositions depending on different local economic developments and responses to global challenges. Nevertheless, the structure of the International Trade Network as a whole remains constant over the years.

We expect that the application of the grand canonical

projection algorithm may reveal deeper structures even in other fields in which bipartite networks are heavily used. In biology, for example, statistically validated projections of mutualistic network of pollinators and plants could uncover interaction patterns among pollinator species due to competition, for which measurements are rarely available and which remain generally unknown [45, 46].

ACKNOWLEDGMENTS

This work was supported by the EU projects Co-eGSS (grant num. 676547), MULTIPLEX (grant num. 317532), Openmaker (grant num. 687941), SoBigData (grant num. 654024) and the FET projects SIMPOL (grant num. 610704), DOLFINS (grant num. 640772). The authors acknowledge Giulio Cimini, Riccardo Di Clemente, Tiziano Squartini and all participants to NEDO Journal Club @IMT for useful discussions.

-
- [1] A. L. Barabási, *Nature Physics* **8**, 14 (2011).
 - [2] G. Caldarelli, *Scale-Free Networks: Complex Webs in Nature and Technology* (Oxford University Press, Oxford (UK), 2010) pp. 1–328.
 - [3] R. Pastor-Satorras and A. Vespignani, *Nature Physics* **6**, 480 (2010).
 - [4] M. Catanzaro and M. Buchanan, *Nature Physics* **9**, 121 (2013).
 - [5] M. O. Jackson, *The Journal of Economic Perspectives* **28**, 3 (2014).
 - [6] S. Battiston, J. D. Farmer, A. Flache, D. Garlaschelli, A. G. Haldane, H. Heesterbeek, C. Hommes, C. Jaeger, R. May, and M. Scheffer, *Science (New York, N.Y.)* **351**, 818 (2016).
 - [7] M. A. Serrano and M. Boguñá, *Physical review. E, Statistical, nonlinear, and soft matter physics* **68**, 015101 (2003).
 - [8] K. Bhattacharya, G. Mukherjee, J. Saramäki, K. Kaski, and S. S. Manna, *Journal of Statistical Mechanics: Theory and Experiment* **2008**, P02002 (2008), [arXiv:0707.4343](https://arxiv.org/abs/0707.4343).
 - [9] M. Barigozzi, G. Fagiolo, and D. Garlaschelli, *Physical Review E* **81**, 046104 (2010).
 - [10] R. Mastrandrea, T. Squartini, G. Fagiolo, and D. Garlaschelli, *Physical Review E - Statistical, Nonlinear, and Soft Matter Physics* **90** (2014), 10.1103/PhysRevE.90.062804, [arXiv:arXiv:1307.2104v2](https://arxiv.org/abs/1307.2104v2).
 - [11] C. A. Hidalgo and R. Hausmann, *Proceedings of the National Academy of Sciences of the United States of America* **106**, 10570 (2009).
 - [12] R. Hausmann and C. A. Hidalgo, *Journal of Economic Growth* **16**, 309 (2011).
 - [13] A. Tacchella, M. Cristelli, G. Caldarelli, A. Gabrielli, and L. Pietronero, *Scientific Reports* **2**, 1 (2012).
 - [14] M. Cristelli, A. Gabrielli, A. Tacchella, G. Caldarelli, and L. Pietronero, *PLoS ONE* **8** (2013).

- [15] C. A. Hidalgo, B. Klinger, A.-L. Barabasi, and R. Hausmann, *Science* **317**, 482 (2007).
- [16] G. Caldarelli, M. Cristelli, A. Gabrielli, L. Pietronero, A. Scala, and A. Tacchella, *PLoS ONE* **7**, 1 (2012), [arXiv:1108.2590](https://arxiv.org/abs/1108.2590).
- [17] A. Zaccaria, M. Cristelli, A. Tacchella, and L. Pietronero, *PLoS ONE* **9**, 1 (2014), [arXiv:1408.2138](https://arxiv.org/abs/1408.2138).
- [18] M. Tumminello, S. Miccichè, F. Lillo, J. Piilo, and R. N. Mantegna, *PLoS ONE* **6** (2011), [10.1371/journal.pone.0017994](https://doi.org/10.1371/journal.pone.0017994), [arXiv:1008.1414](https://arxiv.org/abs/1008.1414).
- [19] S. Gualdi, G. Cimini, K. Primicerio, R. di Clemente, and D. Challet, *Scientific Reports* **6**, 39467 (2016), [arXiv:1603.05914](https://arxiv.org/abs/1603.05914) [q-fin.RM].
- [20] N. Dianati, (2016), [arXiv:1607.01735](https://arxiv.org/abs/1607.01735).
- [21] F. Saracco, M. J. Straka, R. Di Clemente, A. Gabrielli, G. Caldarelli, and T. Squartini, (2016), [arXiv:1607.02481](https://arxiv.org/abs/1607.02481).
- [22] F. Saracco, R. Di Clemente, A. Gabrielli, and T. Squartini, *Scientific reports* **5**, 10595 (2015).
- [23] E. T. Jaynes, *Phys. Rev.* **106**, 620 (1957).
- [24] R. Diestel, *Graph Theory*, Graduate Texts in Mathematics (Springer Berlin Heidelberg, 2017).
- [25] C. Tsallis, in *Phys. D Nonlinear Phenom.*, Vol. 193 (2004) pp. 3–34, [arXiv:0403012](https://arxiv.org/abs/0403012) [cond-mat].
- [26] R. Hanel and S. Thurner, (2011), [10.1209/0295-5075/96/50003](https://doi.org/10.1209/0295-5075/96/50003), [arXiv:1104.2064](https://arxiv.org/abs/1104.2064).
- [27] T. Squartini, E. Ser-Giacomi, D. Garlaschelli, and G. Judge, *PLoS One* **10**, 1 (2015), [arXiv:1501.04759](https://arxiv.org/abs/1501.04759).
- [28] G. Strona, D. Nappo, F. Boccacci, S. Fattorini, and J. San-Miguel-Ayanz, *Nature communications* **5**, 4114 (2014).
- [29] C. J. Carstens, *Physical Review E - Statistical, Nonlinear, and Soft Matter Physics* **91**, 1 (2015).
- [30] P. Deheuvels, M. L. Puri, and S. S. Ralescu, *Journal of Multivariate Analysis* **28**, 282 (1989).
- [31] A. Y. Volkova, *Theory of Probability & Its Applications* **40**, 791 (1996).
- [32] Y. Hong, *Computational Statistics and Data Analysis* **59**, 41 (2013).
- [33] Y. Benjamini and Y. Hochberg, *Journal of the Royal Statistical Society. Series B (Methodological)* **57**, 289 (1995).
- [34] <https://github.com/tsakim/bicm>, <https://github.com/tsakim/bipcm>.
- [35] <http://www.cepii.fr/>.
- [36] B. Balassa, *Manchester School* **33**, 99 (1965).
- [37] F. Saracco, R. Di Clemente, A. Gabrielli, and L. Pietronero, *PLoS ONE* **10** (2015).
- [38] Since the Louvain algorithm depends on the order in which nodes are considered [47], we implemented a more effective version of the original method. The community detection is repeated for several iterations with shuffled node sequence and the community partition giving rise to the highest modularity is eventually kept. The Python code can be found at <https://github.com/tsakim/ShuffledLouvain>.
- [39] F. Saracco, R. Di Clemente, A. Gabrielli, and T. Squartini, *Scientific Reports* **6**, 30286 (2016), [arXiv:1508.03533](https://arxiv.org/abs/1508.03533).
- [40] Icons: ‘Cow’ by Nook Fulloption, ‘Fish’ by Iconic, ‘Excavator’ by Kokota, ‘Light bulb’ by Hopkins, ‘Milk’ by Artem Kovyazin, ‘Curved Pipe’ by Oliviu Stoian, ‘Tractor’ by Iconic, ‘Recycle’ by Agus Purwanto, ‘Experiment’ by Made by Made, ‘Accumulator’ by Aleksandr Vector, ‘Washing Machine’ by Tomas Knopp, ‘Metal’ by Leif Michelsen, ‘Screw’ by Creaticca Creative Agency, ‘Tram’ by Gleb Khorunzhiy, ‘Turbine’ by Leonardo Schneider, ‘Tire’ by Rediffusion, ‘Ball Of Yarn’ by Denis Sazhin, ‘Fabric’ by Oliviu Stoian, ‘Shoe’ by Giuditta Valentina Gentile, ‘Clothing’ by Marvdrock, ‘Candies’ by Creative Mania, ‘Wood Plank’ by Cono Studio Milano, ‘Wood Logs’ by Alice Noir from the Noun Project. All icons are under CC licence.
- [41] C. Tu, J. Carr, and S. Suweis, *PLoS One* **11** (2016), [10.1371/journal.pone.0165941](https://doi.org/10.1371/journal.pone.0165941), [arXiv:1606.01270](https://arxiv.org/abs/1606.01270).
- [42] D. Ricardo, *On the Principles of Political Economy, and Taxation* (J. Murray, 1817).
- [43] T. Squartini, I. van Lelyveld, and D. Garlaschelli, *Scientific reports* **3**, 3357 (2013), [arXiv:rep03357](https://arxiv.org/abs/rep03357) [10.1038].
- [44] Results are independent on the dimensions of the boxes.
- [45] J. Bascombe and P. Jordano, *Annu. Rev. Ecol. Evol. Syst.* **38**, 567 (2007).
- [46] S. Suweis, F. Simini, J. R. Banavar, and A. Maritan, *Nature* **500**, 449 (2013).
- [47] S. Fortunato, *Physics Reports* **486**, 75 (2010), [arXiv:0908.1062](https://arxiv.org/abs/0908.1062).
- [48] J. Park and M. E. J. Newman, *Physical Review E* **70**, 066117 (2004).
- [49] K. Anand and G. Bianconi, *Phys. Rev. E* **80**, 045102 (2009), [arXiv:0907.1514](https://arxiv.org/abs/0907.1514) [cond-mat.dis-nn].
- [50] G. Bianconi, *Phys. Rev. E* **87**, 062806 (2013), [arXiv:1303.4057](https://arxiv.org/abs/1303.4057) [cond-mat.dis-nn].
- [51] P. Erdős and A. Rényi, *Publicationes Mathematicae (Debrecen)* **6**, 290 (1959).
- [52] D. Garlaschelli and M. I. Loffredo, *Physical Review E - Statistical, Nonlinear, and Soft Matter Physics* **78**, 1 (2008), [arXiv:0609015](https://arxiv.org/abs/0609015) [cond-mat].
- [53] T. Squartini and D. Garlaschelli, *New Journal of Physics* **13** (2011), [10.1088/1367-2630/13/8/083001](https://doi.org/10.1088/1367-2630/13/8/083001), [arXiv:1103.0701v2](https://arxiv.org/abs/1103.0701v2).

APPENDIX A: GRAND CANONICAL NULL-MODELS AND NODE SIMILARITY

In the present appendix we revise briefly the methods of [21, 22], making use of the formalism introduced in the section Methods.

Bipartite Null-Models All configuration models of [21, 22] are based on the statistical mechanics approach to complex networks [48–50]; in this framework, the Shannon entropy per graph is defined as

$$S = - \sum_{G_B \in \mathcal{G}_B} P(G_B) \ln P(G_B). \quad (4)$$

Here, \mathcal{G}_B denotes the ensemble of bipartite graphs in which the number of nodes is constant, while the number of links can vary; P is the probability of the bipartite graph G_B belonging to ensemble \mathcal{G}_B . The entropy (4) can be maximized subjected to the vector of constraints $\vec{C}(G_B)$. Solving the entropy maximization in terms of the probability per graph returns

$$P(G_B|\vec{\theta}) = \frac{e^{-\mathcal{H}(\vec{C}(G_B), \vec{\theta})}}{Z(\vec{\theta})}, \quad (5)$$

where $\mathcal{H}(\vec{C}(G_B), \vec{\theta})$ is the Hamiltonian of the system, encoding the constraints. $Z(\vec{\theta}) = \sum_{G_B \in \mathcal{G}_B} e^{-\mathcal{H}(\vec{C}(G_B), \vec{\theta})}$ the partition function and $\vec{\theta}$ is the vector of Lagrangian multipliers associated to the entropy maximization. Different types of null-models can be obtained by modifying the constraints in the Hamiltonian. For instance, by fixing the total number of edges $C = \sum_{i,\alpha} M_{i\alpha} = E$, we obtain the *Bipartite Random Graph* (BiRG), a bipartite version of the well-known Erdős-Rényi model [51]. In accordance with the constraints, its Hamiltonian is given by

$$\mathcal{H}_{\text{BiRG}} = \theta \cdot E. \quad (6)$$

In this case both \vec{C} and $\vec{\theta}$ are scalars, since there is just one condition. In the BiRG model, all edges are equally probable, with probability

$$p_{i\alpha}^{\text{BiRG}} = \frac{e^{-\theta}}{1 + e^{-\theta}} \quad \forall i, \alpha. \quad (7)$$

In the so-called *Bipartite Configuration Model* (BiCM) [22], the degrees of the nodes in both layers are constrained. If k_i and k_α are the degrees respectively for the node i in the Latin layer and for the node α in the Greek layer and θ_i and θ_α the relative Lagrangian multipliers, the Hamiltonian reads thus

$$\mathcal{H}_{\text{BiCM}} = \sum_i \theta_i k_i + \sum_\alpha \theta_\alpha k_\alpha, \quad (8)$$

such that the probability is

$$p_{i\alpha}^{\text{BiCM}} = \frac{e^{-(\theta_i + \theta_\alpha)}}{1 + e^{-(\theta_i + \theta_\alpha)}}. \quad (9)$$

Relaxing the constraints of the BiCM yields the partial Bipartite Configuration Models, BiPCMs, introduced in [21]. In particular, we constrain only the degrees of nodes in one layer. The corresponding Hamiltonians read

$$p_{i\alpha}^{\text{BiPCM}_i} = \frac{e^{-\theta_i}}{1 + e^{-\theta_i}} \quad \forall \alpha \quad (10)$$

$$p_{i\alpha}^{\text{BiPCM}_\alpha} = \frac{e^{-\theta_\alpha}}{1 + e^{-\theta_\alpha}} \quad \forall i. \quad (11)$$

It is worth pointing out that the Hamiltonians for the null-models defined above are all linear in the constraints. In fact the linearity of the constraints permits to express the graph probability $P(G_B)$ in terms of the single link probabilities, i.e. as

$$P(G_B) = \prod_{i,\alpha}^{N_i, N_\alpha} p_{i\alpha}^{m_{i\alpha}} (1 - p_{i\alpha})^{1 - m_{i\alpha}}, \quad (12)$$

for any one of the null-model considered in the present section.

So far equations (7), (9) and (10) are just formal, in the sense that the explicit values of the Lagrangian multipliers θ_i and θ_α are unknown. In order to estimate them, following the strategy of [52, 53], we maximise the Likelihood of the ensemble on the real network. It can be shown that for the BiCM, it reads

$$\begin{cases} \langle k_i \rangle = \sum_\alpha \frac{e^{-(\theta_i + \theta_\alpha)}}{1 + e^{-(\theta_i + \theta_\alpha)}} = k_i^*, \\ \langle k_\alpha \rangle = \sum_i \frac{e^{-(\theta_i + \theta_\alpha)}}{1 + e^{-(\theta_i + \theta_\alpha)}} = k_\alpha^* \end{cases} \quad (13)$$

(starred quantities refers to the real network), such that the Likelihood maximisation is equivalent to impose that the degree sequence expectation values are equal to the values measured on the real network. The expressions for other null-models are analogous. Solving the system of equations (13) allows to calculate the values for all θ_i and θ_α and explicitly obtain the probability per link.

Node Similarity In [21] the similarity measure implemented is just the number of bi-cliques $K_{2,1}$ or $K_{1,2}$ [24] (or V- and Λ -motifs, using the terminology of [22]) existing between two nodes of the same layer. For instance, the number of all V-motifs between i and j , V^{ij} , in the binary bipartite network is therefore given by

$$V^{ij} = \sum_{\alpha \in N_\alpha} M_{i\alpha} M_{j\alpha}. \quad (14)$$

The ‘‘standard’’ approach is to consider the V-motifs as the quantity to analyse; in the approach of [21], the statistical significance of every V^{ij} is stated with reference to the aforementioned null-models in order to reveal relevant node similarities. The monopartite projection includes thus only edges (i, j) whose relative V^{ij} are statistically significant. Since edges are independent (see (12)), the probability of measuring a V-motif consisting of (i, j) on the Latin layer and α on the Greek layer is

$$P(V_\alpha^{ij}) = p_{i\alpha} p_{j\alpha}. \quad (15)$$

In the case of the Random Graph model, for instance, $P(V_\alpha^{ij})_{\text{BiRG}} \equiv (p^{\text{BiRG}})^2 \forall i, j \in N_i, \forall \alpha \in N_\alpha$, since the edge probability is independent of the couple (i, α) and uniform in the network. In this sense, the probability distribution of $V^{ij} = \sum_\alpha V_\alpha^{ij}$ is the sum of independent Bernoulli events, all with the same probability $(p^{\text{BiRG}})^2$, i.e. a Binomial distribution. In the Configuration Model, on the other hand, $p_{i\alpha}$ differs from couple to couple: V^{ij} is thus the sum of independent Bernoulli random variables, in general with different success probabilities. The probability of observing $P(V^{ij} = k)$ will therefore be given by

$$P(V^{ij} = k) = \sum_{\tilde{\alpha}_k \in A_k} \prod_{\alpha \in \tilde{\alpha}_k} P(V_\alpha^{ij}) \prod_{\alpha' \notin \tilde{\alpha}_k} (1 - P(V_{\alpha'}^{ij})) \quad (16)$$

where A_k is the set of all possible choices of k elements from the set $\{1, 2, \dots, N_\alpha\}$ and \bar{a}_k is a single realization, [32].

The Partial Configuration Models are between BiCM and BiRG: the distribution for V^{ij} is the same Poisson Binomial for all couples (i, j) in the case of BiPCM $_\alpha$, while it is a Binomial distribution with probability $p = \frac{k^i k^j}{N_\alpha^2}$ for BiPCM $_i$. In fact, in reconstructing the structure of the V-motifs network it is much more effective to know the degrees of the nodes involved in the V-motifs than the nodes on the other layer, such that the BiPCM $_i$ resulted as more accurate in the network reconstruction. The limits of this intuition are currently under analysis.

Statistical Hypothesis Testing and FDR Validating the statistical significance of the measured V^{ij} therefore revolves around the null hypothesis that its observed value can be explained by the underlying null-model, i.e. that it is compatible with the corresponding probability distribution. For this purpose, we calculate the p -values for right-tailed tests, i.e. $P(V^{ij} \geq V^{*ij})$, where V^{*ij} is the measure on the real network. Note that the total number of distinct couples (i, j) and therefore the number of different hypotheses which are tested simultaneously is $N_i(N_i - 1)/2$. Among other proposals for multiple hypotheses testing, the false discovery rate (FDR) [33] permits a control at each step of the verification procedure. The p -values are ordered according to their values from smallest to largest and label by k . The largest \hat{k} that satisfies

$$p_{value}^{\hat{k}} \leq \frac{\hat{k}\alpha}{N_i(N_i - 1)/2}, \quad (17)$$

defines the effective threshold $p_{th} = \frac{\hat{k}\alpha}{N_i(N_i - 1)/2}$: the hypotheses associated to all p -values smaller than or equal to p_{th} are rejected and are declared as “statistically significant”, i.e. they cannot be explained by the null-model. Once the p -value associated with the couple (i, j) is rejected, in the projected network a binary link is drawn between the two nodes.

APPENDIX B: LIMITS OF THE BiRG AND THE BiPCM $_c$ PROJECTION ON THE PRODUCTS LAYER

The performance of the grand canonical projection algorithm depends on the choice of the null-model, which defines the information of the original bipartite network to be discounted in the link verification process. As already mentioned in the main text, the BiCM imposes the most stringent constraints. For comparison with the BiPCM $_p$ product network, Fig. 9 illustrates the product networks obtained if the BiPCM $_c$ and the BiRG are applied, i.e.

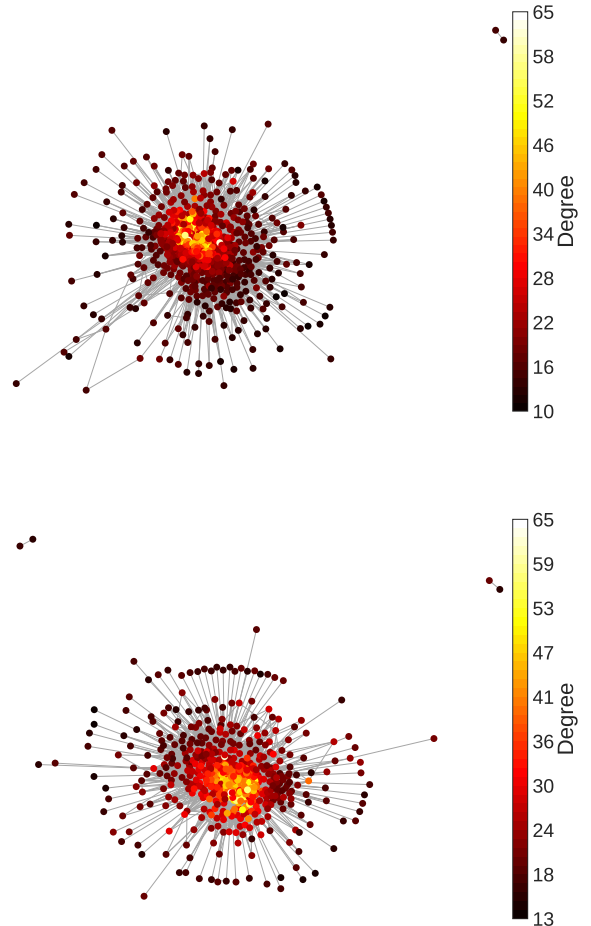


Figure 9: BiRG (top) and BiPCM $_c$ (bottom) product networks for the year 2000. The networks are dominated by the largest connected components whose cores are composed of high degree nodes. The degree values refer to the original country-product bipartite network.

if the nodes of the country layer or the total number of edges are fixed, respectively. It is easy to see that the two are topologically very different from Fig. 5: while the BiPCM $_p$ network is highly fragmented, the BiRG and BiPCM $_c$ networks are dominated by the presence of a large connected component, which contains almost all the nodes. The few isolated clusters are composed of (“meat of swine”, “pig fat”) and (“cocoa paste”, “cocoa butter”), and of (“chromium oxides and hydroxides”, “salts of oxometallic or peroxometallic acids”), respectively. These product couples are thus extraordinarily often exported together compared to others. The difference between the models is also shown in Fig. 10. While the BiRG acts as a relatively “coarse” filter, the statistical verification becomes more strict passing from the BiPCM $_c$ to the BiPCM $_p$ and ultimately to the BiCM, for

which no links are verified. This observation is substantially due to the fact that the node-specific probability distributions of the V^{ij} -motifs collapse into a single distribution for the BiRG and the BiPCM_c, which turn out to be Binomial and Poisson Binomial [21]. Consequently, the null-models induce a one-to-one mapping of the V^{ij} measurements onto the p -values. Imposing a significance level for hypothesis testing amounts therefore to choosing a threshold value $V_{ij,th}$ and discarding motifs with $V_{ij} < V_{ij,th}$. For the BiRG, $V_{ij,th} \in \{9, 10\}$, whereas for the BiPCM_c $V_{ij,th} \in \{12, 13, 14\}$, depending on the year in the interval 1995 - 2010. As a consequence, only products with $V_{ij} \geq V_{ij,th}$ bear significant similarity. The only difference between the motif validations with BiRG and BiPCM_c is a shift in the p -value threshold. The cores of the projection networks host almost exclusively nodes with degrees in the original bipartite network, as one can confirm by closer inspection of Fig. 9. It is worth pointing out that several edges in the BiRG model have p -values which are smaller than the machine precision $\simeq 2.22 \cdot 10^{-16}$.

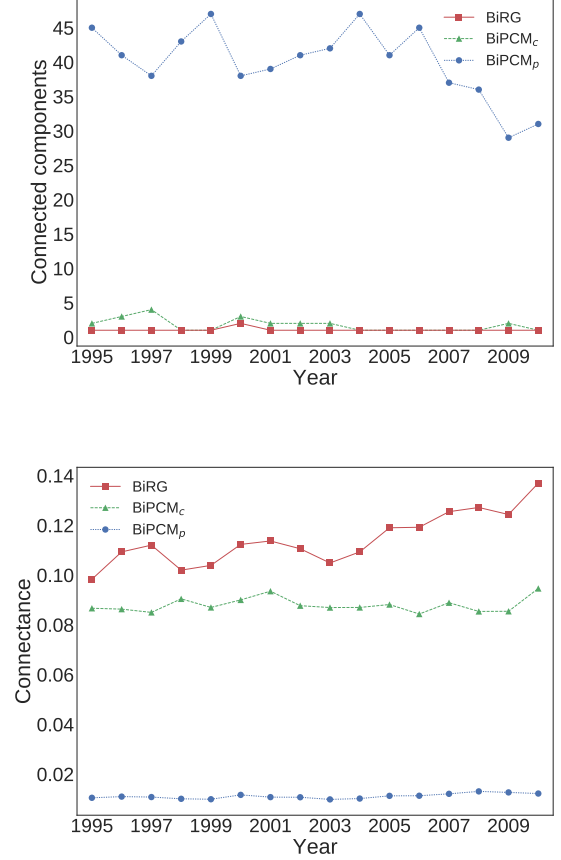


Figure 10: Properties of the product networks spanned by the statistically significant edges according to the respective null-models. The BiPCM_p network is highly fragmented, as shown by the comparatively large number of connected components (top) and the low connectance (bottom). On the other hand, both BiRG and BiPCM_c are composed of comparatively densely connected clusters. Isolated nodes are ignored in both figures.